Inactivation and Degradation of Influenza A Virus on the Surface of Photoactive Self-Cleaning Cotton Fabric Functionalized with Nanocrystalline TiO$_2$

Dmitry Selishchev [1,2,*], Grigory Stepanov [3], Mariia Sergeeva [4], Maria Solovyeva [1,2], Evgenii Zhuravlev [1,3], Andrey Komissarov [4], Vladimir Richter [3] and Denis Kozlov [1,2]

[1] Research and Educational Center "Institute of Chemical Technologies", Novosibirsk State University, Novosibirsk 630090, Russia

[2] Department of Unconventional Catalytic Processes, Boreskov Institute of Catalysis, Siberian Branch, Russian Academy of Sciences, Novosibirsk 630090, Russia

[3] Institute of Chemical Biology and Fundamental Medicine, Siberian Branch, Russian Academy of Sciences, Novosibirsk 630090, Russia

[4] Smorodintsev Research Institute of Influenza, Ministry of Health of the Russian Federation, Saint-Petersburg 197376, Russia

[*] Correspondence: selishev@catalysis.ru; Tel.: +7-3833269429

Abstract: Chemical modification of cotton-rich fabrics with TiO$_2$ nanoparticles results in photoactive self-cleaning textiles, which can provide, under UV or solar radiation, complete oxidation of low-molecular compounds, degradation of supramolecular structures, and inactivation of microorganisms due to the photocatalytic effect. In this paper, we describe, based on the example of influenza A (H1N1) virus, a photoinduced antiviral effect of cotton fabric functionalized with nanocrystalline TiO$_2$. Fast inactivation of influenza virus occurs on the irradiated surface of photoactive fabric due to adsorption and photocatalytic degradation. The TiO$_2$ component in the prepared fabric increases the adsorption effect compared to initial cotton due to a high specific area of TiO$_2$ nanocrystallites. Long-term irradiation leads to destruction of all virion structures to the point of RNA molecules. In contrast to pristine cotton, no virus RNA is detected using the polymerase chain reaction (PCR) technique after long-term irradiation of photoactive fabric. The results of this study underline the potential of photoactive self-cleaning fabrics for application in air purification systems and personal protective clothes to provide permanent protection of people against harmful chemical and biological pollutants.

Keywords: TiO$_2$ photocatalyst; self-cleaning textile; photoactive cotton; influenza virus; antiviral properties; RNA degradation

1. Introduction

Self-cleaning materials and coatings for elements of urban infrastructure, exterior and interior of buildings, and special products are actively used to provide permanent protection of people against harmful chemical and biological pollutants in social places [1–3]. Recently, the worldwide pandemic due to COVID-19 (SARS-CoV-2 coronavirus) has underlined the need for improving and expanding these technologies to reduce the spread of dangerous diseases.

Self-cleaning fabrics prepared by functionalization of natural [4,5] and synthetic [6] fibers using various modifiers comprise an important portion of self-cleaning materials and can be used as textiles to produce personal protection clothes or as fabric filters for air purification systems [1,7]. Cotton is the most used textile substrate for modification due to the extended surface of cotton fibers resulting in better adhesion of modifiers.

Silver and copper nanoparticles are well-known modifiers that provide antibacterial properties for fabrics [8,9]. Graphene oxide [10], chitosan and its derivatives [11], quaternary ammonium compounds [12], and triclosan [13] can also be used for this purpose. Another type of modifier is semiconducting photocatalysts: for instance, TiO_2, ZnO, WO_3, and their composites [3,14,15]. Photoinduced self-cleaning and antimicrobial properties are observed for fabrics modified with photocatalysts, especially with TiO_2 of anatase structure because it is the most active and stable photocatalyst for oxidative degradation in oxygen-contained medium [16]. In addition to photocatalytic degradation for environmental protection, TiO_2 is commonly used in other photocatalytic processes, including photocatalytic hydrogen production [17,18], CO_2 reduction [19,20], and photoelectrochemical conversion [17,21,22]. The preparation technique strongly affects the properties of TiO_2 and its photocatalytic activity [23,24]. Typically, high values of activity are achieved in the case of nanocrystalline form of TiO_2 due to a short distance for diffusion of photogenerated charge carriers from volume to the surface of TiO_2 nanocrystallites, as well as an extended surface with a high number of sites available for adsorption of molecules and interfacial charge transfer [25]. Nanocrystalline TiO_2 can be anchored on the external surface of nonporous and porous supports (e.g., glasses [26], adsorbents [27,28], polymeric fibers [29], and fabrics [7,30]) to prepare composites with enhanced properties or functional materials.

Fabrics functionalized with nanocrystalline photocatalysts can completely decompose low-molecular compounds due to formation of reactive oxygen species under corresponding radiation. In the case of TiO_2, OH-radicals are regarded as the main species that provides oxidation reactions. Degradation of formaldehyde [31], acetone [32], phenol [33], and gaseous ammonia [34] over photoactive fabrics was previously investigated and described. High-molecular organic compounds can also be degraded on the irradiated surface of functionalized fabrics. The conventional method to evaluate the activity of photoactive fabrics is discoloration of spots under radiation. Organic dyes [35], coffee [36], wine [35,37], juice [38], make-up, and sweat [39] were used for this purpose. The activity is typically measured as a change in color of material compared to the reference sample without the photocatalyst. Complete discoloration of spots can be achieved on the surface of photoactive fabrics after long-term irradiation.

In addition to degradation of chemical compounds, the photoactive component of self-cleaning fabrics can lead to degradation of membranes and cell walls of various microorganisms (e.g., protozoa, bacteria, endospores, fungi, and algae), resulting in their death [3,40]. Many researchers focus on development of materials to kill bacteria efficiently [41]. The antibacterial properties of photoactive fabrics were typically tested using Gram-negative bacteria *Escherichia coli* [38,42] and Gram-positive bacteria *Staphylococcus aureus* [43] based on the AATCC test method 100. Other types of bacteria (e.g., *Micrococcus luteus* [44], *Pseudomonas fluorescens* [45], and *Klebsiella pneumoniae* [46]) were less common. Under irradiation, faster inactivation of bacteria typically occurs on the surface of photoactive fabrics compared to the initial textile substrates. Although the details regarding the mechanism of bacterium degradation are still under discussion, the main pathways are well described in the literature [47]. Fungi can also be degraded over photoactive fabrics. *Candida albicans* [43] and *Aspergius niger* [48] fungi were used to evaluate the antifungal activity of textile materials. Typically, degradation of fungi is substantially slower compared to degradation of bacteria due to fungi having a thicker cell wall [49].

Concerning viruses, which exhibit an increased impact on human health and safety nowadays, investigation of these types of biological contaminants on surfaces of photoactive textile materials has received less attention. At the same time, TiO_2-based photocatalysts are known to be able to inactivate viruses under UV irradiation. For instance, influenza A virus was inactivated in an aqueous suspension of TiO_2 [50] on the surface of glass covered with a thin film of TiO_2 [51,52], composite [53], and functionalized cotton [54,55]. Virus inactivation was evident using the 50% tissue culture infective dose (TCID50) method [56,57] or plaque assay method [58,59]. Sodium dodecyl sulfate poly-

acrylamide gel electrophoresis (SDS-PAGE) was used to confirm the degradation of viral proteins [56]. Destruction of virus structures during photocatalytic treatment was also confirmed by the polymer chain reaction (PCR) technique followed by electrophoresis using agarose gel [54]. Therefore, irradiated photocatalyst promotes destruction of virions due to formation of reactive oxygen species.

Photoinduced antiviral activity of TiO_2 was also demonstrated for other viruses (e.g., herpes simplex virus [60], feline calicivirus [58], murine norovirus [61], rotavirus [62], and astrovirus [62]) and bacteriophages (e.g., MS2 [61,63], T4 [64], Qβ [64,65], and f2 [66]). All these viral contaminants were inactivated under long-term irradiation. These studies allow us to assume a similar effect for self-cleaning fabrics functionalized with nanocrystalline TiO_2. The main questions are related to evaluation of the time required for complete inactivation of viruses and the products of their degradation. It was our motivation to perform this study.

In this study, we aimed to investigate inactivation and further degradation of influenza A virus on the irradiated surface of highly active and stable photocatalytic textile material prepared via modification of cotton fabric using the impregnating compound based on titanium (IV) isopropoxide precursor and nanocrystalline TiO_2. Influenza virus was selected due to this RNA-based enveloped virus causing annual seasonal epidemics or even pandemics [67]. We also believe that the results of this study would be helpful for further investigation of other dangerous RNA-based enveloped viruses (e.g., SARS-CoV-2 coronavirus).

2. Results and Discussion

In this study, cotton fabric was functionalized with nanocrystalline TiO_2 to prepare a photoactive textile material. The photocatalytic ability of the prepared material was evaluated in degradation of acetone vapor and influenza A virus under UV-A irradiation.

2.1. Characteristics of Photoactive Fabric

The preparation technique using an alcohol solution of titanium isopropoxide with addition of nanocrystalline TiO_2 resulted in deposition and fixation of TiO_2 particles on the surface of cotton fibers. The total content of Ti measured using the ICP-MS method in the prepared material after the washing procedure was 0.87 wt.%, which corresponds to a high value. This value was achieved due to using titanium isopropoxide as a binding agent, which formed, after hydrolysis, an amorphous matrix and provided adhesion of TiO_2 nanoparticles to the cotton surface. The SEM micrographs in Figure 1a,b illustrate a change in the morphology of cotton fibers after functionalization, when evenly distributed TiO_2 particles can be found on the smooth external surface of cotton fibers. Because the material was used after washing in an automated washing machine, only strongly attached TiO_2 particles remained on the surface of cotton fibers, and no aggregation of these particles was detected during SEM analysis, even at a high accelerating voltage. Figure 1c,d shows a local structure of these particles. They are agglomerates with sizes up to 1 μm consisting of aggregated TiO_2 nanoparticles.

The XRD method was used to check the crystal phase of attached TiO_2. Figure 2a shows the XRD patterns of the initial cotton fabric and prepared material. Pristine cotton exhibited a typical XRD pattern with four main peaks at 14.9°, 16.5°, 22.7°, and 34.1°. Based on literature data [68], these peaks can be attributed to the (1–10), (110), (200), and (004) diffraction planes of cellulose Iβ, respectively. Attachment of TiO_2 after functionalization of the cotton fabric led to the appearance of additional peaks and a simultaneous decrease in the intensity of peaks attributed to cellulose because Ti has a higher atomic weight than C, H, and O. According to JCPDS card No. 21-1272, a marked peak at 25.3° and other peaks at 37.8°, 48.0°, 53.9°, and 55.1° in the XRD pattern of the photoactive fabric correspond to anatase TiO_2 and can be attributed to the (101), (004), (200), (105), and (211) diffraction planes of anatase, respectively [69,70]. This confirms the crystal structure of anatase for the TiO_2 particles attached to the cotton fibers. An averaged size of TiO_2 crystallites

estimated using the Scherrer equation was 12 nm, which is close to the value for the starting TiO_2 source (i.e., TiO_2 Hombikat UV 100) and confirms the nanocrystalline form of attached TiO_2.
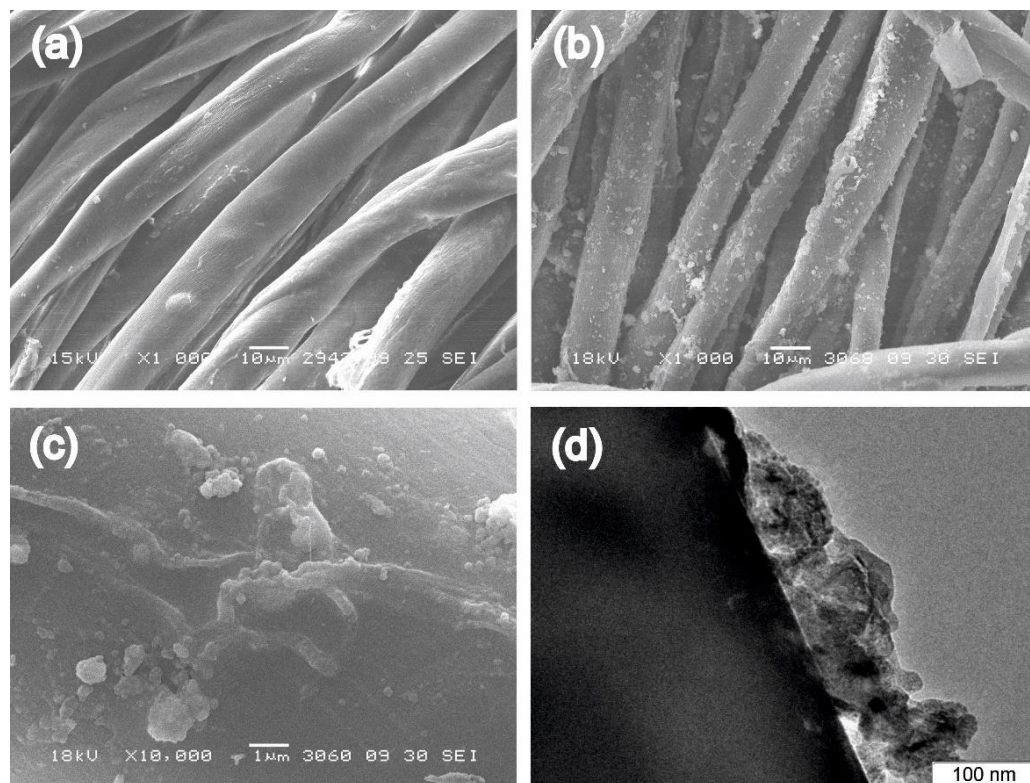
Figure 1. SEM images of initial cotton (**a**) and cotton functionalized with nanocrystalline TiO_2 (**b,c**); TEM cross-view image of cotton fiber with attached TiO_2 particles (**d**).
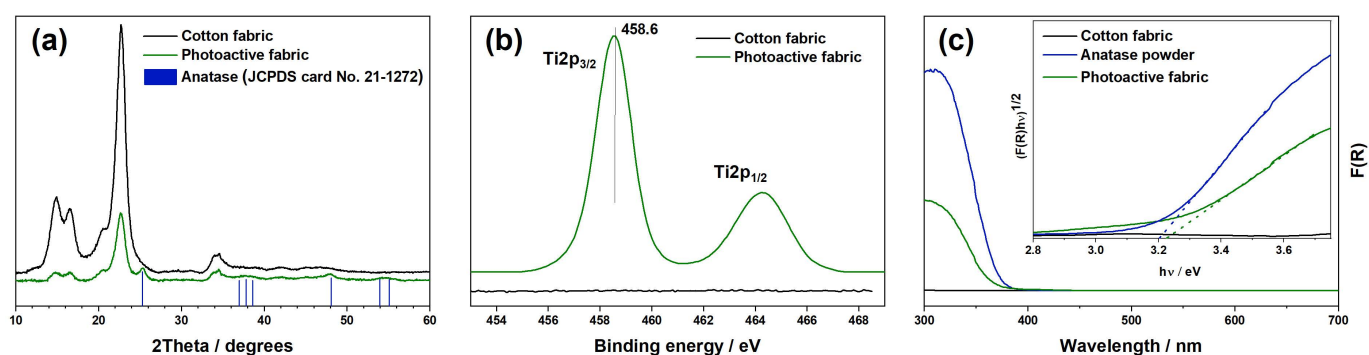
Figure 2. XRD patterns (**a**), X-ray photoelectron spectra (**b**), and UV-Vis absorbance spectra (**c**) of pristine cotton fabric and prepared photoactive fabric. The inset in (**c**) shows corresponding Tauc plots.

XPS analysis also confirmed the presence of titanium on the surface of functionalized fabric. A binding energy of 458.6 eV for the Ti2p3/2 peak in Ti2p photoelectron spectral region (Figure 2b) indicates the charge state of +4 for titanium in the case of photoactive fabric, which agrees with the results of the XRD analysis.

Functionalization of the cotton fabric led to a change in its optical properties. In contrast to the initial cotton, strong absorption of light in the UV region was observed for the TiO_2-modified fabric (Figure 2c). This absorption is due to the interband excitation of electrons in TiO_2 nanocrystallites attached to the surface of cotton fibers. Estimation of the optical band gap for photoactive fabric using the Tauc method (see the inset in

Figure 2c) provided a value of 3.22 eV, which corresponds well to the bang gap of starting anatase TiO_2 Hombikat UV 100 powder (3.20 eV) and other anatase photocatalysts [25]. Therefore, generation of charge carriers (i.e., electron and hole) can occur in photoactive fabric under radiation with wavelengths shorter than 385 nm. The photogenerated charge carriers can further interact with electron donors or acceptors and form on the surface of TiO_2 nanocrystallites' reactive oxygen species, which are able to decompose organic contaminants.

All the characterization methods confirm the presence of TiO_2 in the prepared material. As the photocatalytically active nanocrystalline TiO_2 was used in the impregnating compound during synthesis, the prepared material is expected to exhibit high photocatalytic activity under UV radiation. To check this activity and to evaluate its ability for degradation of contaminants, it was tested regarding oxidation of acetone vapor in the continuous flow setup. Similar to powdered TiO_2 photocatalysts [71], the prepared photoactive fabric is able to completely oxidize acetone vapor under UV-A radiation. Carbon oxides and water were the final oxidation products, and no formation of gaseous organic intermediates was detected during the test. At a radiation power of 9.7 mW·cm^{-2}, the steady-state rate of CO_2 formation during the oxidation of acetone was 0.74 ± 0.4 μmol·min^{-1}, which corresponds to high photocatalytic activity. To provide a reference for other researchers, we also tested under the same conditions TiO_2 P25 from Evonik Ind. (Germany), which is a well-known and commonly used photocatalyst for oxidation reactions. The steady-state rate of CO_2 formation over a layer of TiO_2 P25 (ca. 30 mg·cm^{-2}) was 1.24 μmol·min^{-1}. This result indicates that the prepared photoactive fabric has high photocatalytic activity in the degradation of organic compounds, which is comparable to the activity of powdered photocatalysts. The material also had high stability under long-term irradiation because a similar level of activity was observed for a long time during the tests.

In addition to low-molecular organic compounds, the prepared material was able to decompose the supramolecular structures and microorganisms. The sections below describe the results on inactivation and degradation of influenza A virus on the irradiated surface of the prepared photoactive fabric.

2.2. Inactivation of Influenza Virus

The effects of time and irradiation with UV light on the infectivity of influenza virus deposited on the surface of cotton and photoactive fabrics were investigated using the TCID$_{50}$ method.

Figure 3 shows the kinetic plots of infectivity for each material with and without UV irradiation. After deposition of virus suspension on the surface of both cotton and photoactive fabrics (i.e., time point of 0 min), its titer was substantially decreased compared to the initial value (i.e., inoculum) due to adsorption of virus particles into fabrics. This effect is due to a high adsorption ability of used cotton substrate, which had an area density of 350 g·m^{-2}. At the same time, a decrease in the concentration of total protein in the initial virus suspension from 10 to 0.2 mg·mL^{-1} led to an increase in the initial adsorption of virus particles because lower values of virus titer were detected in this case (Figure 3c, 0 min). This occurred due to the fact that, at lower concentrations, protein molecules from allantoic fluid (mainly albumin) competed less with virus particles for adsorption sites, and a higher number of virus particles were strongly adsorbed on the surface of materials. Under these conditions, the TiO_2 component in the prepared photoactive fabric increased the adsorption effect compared to the initial cotton due to a high specific area of attached TiO_2 nanocrystallites (Figure 3c).
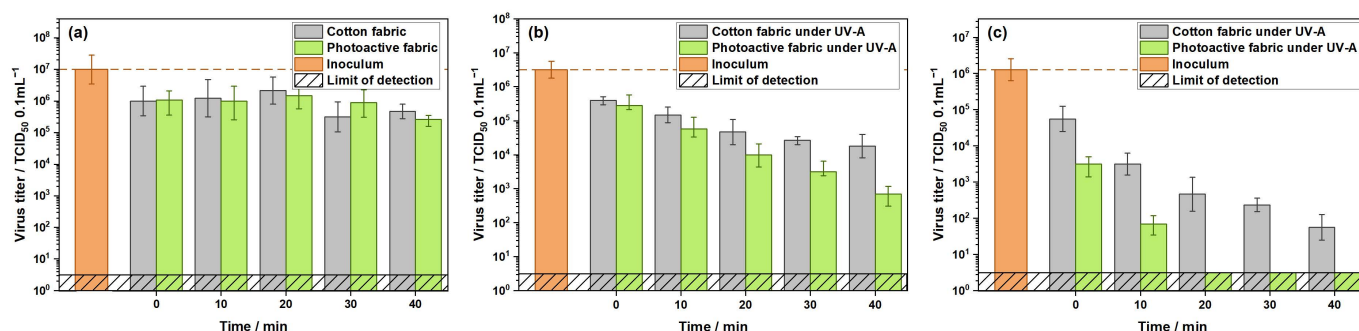
Figure 3. Dependence of virus titer on incubation time of contaminated cotton and photoactive fabrics without (**a**) and with (**b**,**c**) UV irradiation. Concentration of total protein in inoculum corresponds to 10 and 0.2 mg·mL^{-1} for (**a**,**b**) and (**c**), respectively.

It is also important to note that a much higher adsorption effect for the studied materials was observed in the case of *E. coli* bacteria, when ca. 90% of the cells from the initial suspension were adsorbed on the surface of cotton or photoactive fabrics after 15 min (see Figure S1 in the Supplementary Materials). These data indicate strong adsorption capacity of cotton-rich materials and show that they are a good substrate for accumulation of viruses and bacteria. Nanocrystalline TiO$_2$ used as a modifier for functionalization of cotton-rich fabrics can substantially increase the adsorption capacity of the materials.

Figure 3a shows that long-term incubation of contaminated cotton and photoactive fabrics without UV irradiation had no strong effect on the infectivity of the deposited virus because, for both materials, a similar level of virus titer was detected for 40 min. These data confirm the stability of the influenza virus under the mentioned conditions.

Irradiation of both materials with UV-A light led to a monotonic decrease in the virus titer (Figure 3b). In the case of cotton fabric, the rate of inactivation gradually decreased during irradiation, while, for the photoactive fabric, a linear decrease in virus titer was observed at the mentioned period. As will be discussed below, small differences between cotton and photoactive fabrics under irradiation for the first 10 to 20 min are related to a stabilization effect by protein, which had a high concentration in this case. After 40 min of irradiation, the value of virus titer for the photoactive fabric was 25 times lower than the corresponding value for the initial cotton.

UV radiation of A region is known to have a lower impact on the stability and infectivity of the virus compared to UV radiation of B and C regions [61,72]. Heating of textile samples occurred under continuous irradiation with UV-LED, and, probably, it was one of the reasons for the decrease in the infectivity of the virus deposited on the irradiated surface of the cotton fabric (Figure 3b). In the case of the photoactive fabric, the rate of inactivation under UV was higher than for the initial cotton due to photocatalytic degradation of the virus particles using reactive oxygen species formed on the irradiated TiO$_2$ particles. Oxidation of the external proteins, destruction of the capsid and envelope, and decomposition of the internal molecules can occur during TiO$_2$-mediated photocatalytic degradation of virus particles [72]. These pathways are responsible for inactivation of a virus and for the decrease in its infectivity.

Long-term irradiation with UV-A light led to complete inactivation of the influenza virus on the surface of the studied materials. In the case of photoactive fabric, the limit of detection was reached after 100 min of irradiation (Figure S2). For the cotton fabric, the measured value of virus titer at the same period was $10^{1.6} = 40$ TCID$_{50}$ 0.1 mL^{-1}, and extra time was required for complete inactivation of the virus in this case. Therefore, the cotton fabric functionalized with nanocrystalline TiO$_2$ results in faster inactivation of influenza A virus compared to the initial cotton.

It is important to note that the effect of UV-A light on inactivation of influenza virus on the surface of photoactive and cotton fabrics depends on the composition of the initial virus suspension. Based on our experience, the total concentration of proteins in the nasal

secretions of people is varied in a broad range, typically 0.2 to 8 mg·mL^{-1}. Therefore, in addition to the experiments described above with the virus suspension initially containing 10 mg·mL^{-1} of total protein, which could affect the stabilization of the virus, we also conducted the experiments with its low concentration to investigate the effect of composition on the kinetics of inactivation. A decrease in the concentration of protein from 10 to 0.2 mg·mL^{-1} led to an increase in the initial adsorption of the virus on the surface of materials, as described above, and to a substantial increase in the rate of virus inactivation (Figure 3c). For these conditions, the limit of detection in the case of photoactive fabric was reached for less than 20 min of irradiation, while, for the initial cotton virus, the particles were infectious even after 40 min. TiO$_2$-mediated photocatalytic oxidation is driven by photogenerated reactive oxygen species (mainly OH-radicals) and has no strong specificity to the type of contaminants, including chemical compounds and biological objects [41]. As a result, all organic matter can be degraded by reactive oxygen species formed on the irradiated surface of TiO$_2$ particles. At a lower concentration of protein, a higher number of photogenerated active species interact directly with virus particles, and faster inactivation of the virus occurs compared to the virus suspension containing a great deal of organic matter. It should be noted that, in the case of a low concentration of protein, the influenza virus itself was less stable because a higher rate of its inactivation was observed on the surface of the initial cotton under these conditions compared to the virus suspension containing 10 mg·mL^{-1} of protein.

Therefore, functionalization of cotton fabric with nanocrystalline TiO$_2$ results in photoactive self-cleaning material, which can quickly adsorb influenza virus and inactivate it under UV-A irradiation. A further question was related to the possibility for complete decomposition of virus particles to prevent its accumulation into fabric.

2.3. Degradation of Influenza Virus

In addition to TCID$_{50}$ analysis, which is conventional for studies on inactivation of viruses, we employed the RT-qPCR technique to illustrate the decomposition of virus particles on the surface of prepared photoactive fabric. RT-qPCR is a method based on synthesis of the complementary DNA from the target RNA template followed by doubling the target DNA fragment in each cycle of PCR. It enables precise detection of RNA in fluids. Photocatalytic degradation of RNA molecules via oxidation of the nitrogen bases or destruction of the RNA chain would affect the response during PCR analysis.

We also used influenza virus A/PR/8/34 (H1N1) for these experiments, but it was suspended in a culture medium. According to the threshold cycle value Cq during PCR tests, the concentration of the used virus suspension was similar to the concentration of virus in nasopharyngeal swabs from infected patients.

The initial cotton and prepared photoactive fabric were contaminated with the culture medium containing influenza A virus and irradiated with UV-A for several time periods, followed by RT-qPCR analysis. Similar experiments without UV irradiation were also performed to check the stability of the virus on the surface of materials. Figure 4a shows the threshold cycle values Cq for the initial virus suspension and washouts from the textile samples to illustrate the effects of the material and UV irradiation. Different behavior under irradiation was observed for the initial cotton and prepared photoactive fabric. In contrast to both materials without irradiation and irradiated cotton fabric, a trend for increasing Cq value with increasing the time of UV irradiation was observed for the prepared photoactive fabric only. As briefly described in the experimental section, a higher Cq value corresponds to a lower concentration of virus RNA in the analyzed probe. After 3–6 h of irradiation, the Cq value for photoactive fabric reached the detection limit that corresponded to the level of response for the culture medium without virus (Figure 4a). This result indicates that, in contrast to the initial cotton, destruction of all the RNA molecules occurred on the surface of the photoactive fabric under long-term irradiation with UV-A light. The genetic material of influenza virus (i.e., RNA molecules) is protected with a capsid and an envelope. The destruction of RNA molecules caused by photocatalytic oxidation on the surface of

TiO$_2$-mediated fabric means that the degradation of the envelope lipid bilayer and matrix protein layer of virions has occurred before that. Therefore, it confirms the mechanism of photoinduced antiviral activity of cotton fabric functionalized with nanocrystalline TiO$_2$ via the complete destruction of virion.
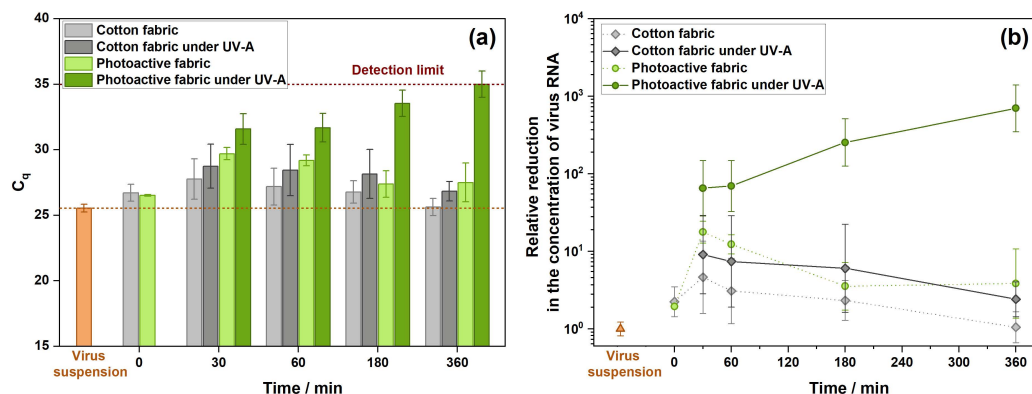
Figure 4. PCR data on threshold cycle values Cq (**a**) and normalized concentration of virus RNA (**b**) for initial virus suspension and washouts from the textile samples.

The calculation technique, when the data for each time were normalized to the value for initial virus suspension, was employed to illustrate a change in the concentration of viral RNA molecules and to clearly discuss the effect of material and UV-A light (Figure 4b). A decrease of two times in the concentration of viral RNA compared to the initial suspension was observed for the time point of 0 min, which corresponds to the analysis of washouts immediately after dropping the culture-medium-contained virus on the surface of materials. This effect is due to fast and strong adsorption of virus particles on the surface of textile materials, which prevents the washing out and detection of RNA molecules. It is similar to the results on virus inactivation, when the virus titer was substantially decreased after dropping the suspension on the materials (Figure 3).

Incubation of initial and photoactive cotton samples contaminated with virus for 30 min without irradiation resulted in a further decrease in the concentration of viral RNA detected in washouts (up to 17 times). This decrease can also be caused by further adsorption of virus particles on the material surface. As the used cotton substrate had a high area density (i.e., 350 g·m^{-2}), a long time for achievement of adsorption–desorption equilibrium was required. Additionally, the TiO$_2$ component in the prepared photoactive fabric also increased the adsorption effect due to a high specific area of attached TiO$_2$ nanocrystallites. As a confirmation of the statements made above, the Supplementary Materials contain data on the adsorption kinetics of *E. coli* bacteria on the surface of cotton and photoactive fabrics (Figure S1). Adsorption of *E. coli* monotonically increased during incubation without irradiation until almost all the cells were adsorbed on the surface of materials after 1 h.

Under longer incubation of initial and photoactive cotton samples contaminated with virus without irradiation, a small increase in the concentration of viral RNA detected in washouts was observed compared to the time point of 30 min. Probably, a partial destruction of virus particles adsorbed on the surface of materials occurred, which resulted in an extraction of additional RNA molecules in liquid medium.

UV-irradiated cotton fabric contaminated with virus had the same trend. No decrease in the concentration of virus RNA was observed for the initial cotton under long-term irradiation. As stated above, only UV-irradiated cotton fabric modified with nanocrystalline TiO$_2$ led to a monotonic decrease in the concentration of RNA molecules due to their photocatalytic degradation. If compared to the initial virus suspension, the concentration of RNA molecules was decreased by 700 times after 6 h of irradiation. As shown in Figure 4a, the detection limit of the PCR technique for this system was achieved after this time. Based on these data and the results of previous studies [56,73], it can be concluded that

nanocrystalline TiO_2 in the composition of photoactive material decomposes virus particles under irradiation with UV-A light, with the destruction of the lipid bilayer of the envelope, protein content, and genetic material of the virus (Figure 5). Long-term irradiation resulted in the decomposition of RNA molecules to fragments, with the number of nucleotides lower than 100 not to be detected using the PCR technique because the primers used for amplification flanked a sequence of ca. 100 nucleotides. This behavior (i.e., degradation of biological agent with gradual decomposition of all its structures to smallest fragments) is similar to the complete oxidation of low-molecular organic compounds to carbon oxides and water (i.e., mineralization).
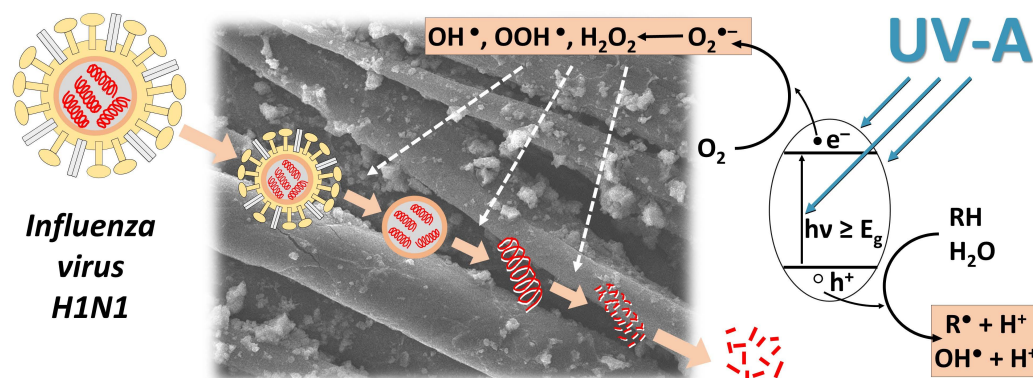
Figure 5. Scheme of virus degradation on the irradiated surface of photoactive cotton fabric.

Therefore, the results discussed above show that functionalization of cotton fabric with nanocrystalline TiO_2 provides self-cleaning textile material with photoinduced antiviral properties, which can quickly adsorb, inactivate, and completely decompose influenza virus under UV-A irradiation.

Application of the visible-light-active TiO_2 component in the proposed preparation technique would extend the photoresponse of as-prepared material to the visible region of the spectrum and also provide inactivation of virus contaminants under visible light. For instance, TiO_2 can be doped with nitrogen (TiO_2-N), and the impurity energy levels of nitrogen created in the band gap of TiO_2 would lead to a decrease in the minimum energy required for photoexcitation of electrons from 3.2 eV for pristine TiO_2 to 2.3 eV for formed TiO_2-N, which corresponds to a shift in the absorption edge to the visible region of the spectrum [74]. Similar to the data presented in Section 2.3 (Figure 4b), irradiation of cotton-rich fabric, which was functionalized using TiO_2-N with blue light (450 nm), led to a monotonic decrease in the concentration of RNA molecules of influenza virus, which also confirms the possibility to decompose virus particles under visible light (see Figure S3 in Supplementary Materials). This short remark underlines the potential of personal protective clothes made from photoactive self-cleaning fabrics for daily use to provide permanent protection against viruses and other contaminants.

3. Materials and Methods

3.1. Preparation and Characterization of Photoactive Fabric

Bleached cotton fabric with an area density of 350 g·m^{-2} was used as a textile substrate for modification with TiO_2 to provide self-cleaning properties. Modification of cotton fabric was performed via the impregnation method using titanium (IV) isopropoxide ($Ti(OC_3H_7)_4$; >98%; Acros Organics, Morris Plains, NJ, USA) precursor and photoactive nanocrystalline TiO_2 according to our previously published technique [75]. A commercial photocatalyst TiO_2 Hombikat UV 100 (100% anatase, ~10 nm crystallites) from Sachtleben Chemie GmbH (Duisburg, Germany) was used as a photoactive component. Briefly, the textile samples were obtained via impregnation of washed cotton pieces with a size of 9 × 9 cm^2 using the suspension of $Ti(OC_3H_7)_4$ and milled TiO_2 (10 g·L^{-1}) in isopropyl alcohol (AO Reachem Inc., Moscow, Russia) followed by treatment with water steam and drying in air at 110 °C.

Then, a typical home washing procedure at 40 °C for 30 min was performed using an automated washing machine to remove poorly attached TiO_2 particles. Finally, the samples were thoroughly rinsed with deionized water and dried in air at an increased temperature.

Ti content in the prepared samples was measured by inductively coupled plasma-mass spectrometry (ICP-MS) using an Agilent 7700 spectrometer (Agilent, Palo Alto, CA, USA). The morphology of initial cotton and TiO_2-modified photoactive fabric was studied by scanning electron microscopy (SEM) using a JSM-6460 LV microscope (JEOL, Tokyo, Japan) at 15–18 kV and by transmission electron microscopy (TEM) using a JEOL-2010 microscope (JEOL) at 200 kV. The crystal phase of attached TiO_2 was analyzed by XRD using a D8 Advance diffractometer (Bruker, Billerica, MA, USA) equipped with a $CuK\alpha$ radiation source and a LynxEye position sensitive detector. Chemical state of titanium was studied by X-ray photoelectron spectroscopy (XPS) using an ES300 spectrometer (Kratos Analytical, Manchester, UK) equipped with a $MgK\alpha$ ($h\nu$ = 1253.6 eV, 170 W) radiation source. The spectrometer was calibrated using $Au4f_{7/2}$ and $Cu2p_{3/2}$ photoelectron lines of bulk gold and copper foil with a binding energy (BE) of 84.0 and 932.7 eV, respectively. The UV–Vis diffuse reflectance spectra for initial cotton fabric and prepared photoactive material were recorded at room temperature using a Cary 300 UV–Vis spectrophotometer from Agilent equipped with a DRA-30I diffuse reflectance accessory in the range of 300–700 nm with a resolution of 1 nm. Special prepacked polytetrafluoroethylene from Agilent was used as a reflectance standard. The diffuse reflectance spectra were recalculated to an absorbance mode using the Kubelka-Munk function. Optical band gap was estimated using the Tauc method based on the assumption of allowed indirect transitions.

To check the photocatalytic activity of prepared material in the degradation of organic compounds, it was tested in the oxidation of acetone vapor under UV-A radiation in a continuous-flow setup. This setup was previously used for the investigation of functional properties of various TiO_2-based photocatalysts, and the details can be found in our previously published paper [76]. For the experiments, small pieces with an area of 9 cm^2 were cut from the prepared material and placed into a photoreactor. A 10-W UV-light-emitting diode (LED) was used for irradiation of the samples. According to measurements using an ILT 950 spectroradiometer (International Light Technology, Peabody, MA, USA), LED provided the radiation with a specific power of 9.7 mW·cm^{-2} and a maximum at 371 nm (i.e., UV-A region).

3.2. Analysis of Virus Inactivation Using $TCID_{50}$ Technique

Influenza virus A/PR/8/34 (H1N1) from the virus collection of the Smorodintsev Research Institute of Influenza (Saint-Petersburg, Russia) was selected for the investigation of photoinduced antiviral activity of the prepared material. For these experiments, small pieces with an area of 2 cm^2 were cut from photoactive fabric, autoclaved at 121 °C for 40 min for sterilization, and placed in Petri dishes. Initial cotton fabric was used as a control by the same method to evaluate the effect of functionalization. A 50-µL aliquot of virus containing allantoic fluid with 10 mg·mL^{-1} of total protein measured using Quant-It Protein Assay Kit or its suspension (1:50) in Dulbecco's phosphate-buffered saline (DPBS; Biolot, Saint-Petersburg, Russia) was dropped on each piece of photoactive material or cotton fabric. The concentration of total protein in diluted virus suspension was 0.2 mg·mL^{-1}. Petri dishes with contaminated samples were covered with quartz glasses to prevent evaporation of liquid and were irradiated using a 100-W UV-LED for 10, 20, 30, or 40 min to analyze the kinetics of inactivation for each textile material. According to measurements using an ILT 950 spectroradiometer), LED provided radiation with a specific power of 8.0 mW·cm^{-2} and a maximum at 367 nm (i.e., UV-A region). Similar experiments without UV irradiation were also performed to check the stability of virus. After time mentioned above, the samples were immersed into 2 mL of cold DPBS and vigorously shaken to rinse out the virus from the surface of fabrics. The control point without irradiation (i.e., 0 min), when the samples were immersed into 2 mL of cold DPBS immediately after dropping the suspension of virus on their surface, was performed to check the effect of adsorption of

virus on the textile substrate. At least three repeats were performed for each irradiation time for both materials.

All washouts from the contaminated samples were stored on ice during the day of experiment. The concentration of infectious virus was quantitated by $TCID_{50}$ method using MDCK cells (IRR #FR-58). Briefly, series of 10-fold dilutions of initial virus suspension and washouts from the samples were made in AlphaMEM culture medium (Biolot) supplemented with TPCK trypsin (2 µg mL^{-1}; Sigma Aldrich, St. Louis, MO, USA), HEPES (25 mM; Sigma Aldrich), and BSA (0.2%; Sigma Aldrich). Confluent MDCK cells in 96-well plates (TPP) were washed twice with DPBS and inoculated with 0.1 mL of the prepared dilutions. After incubation period (3 days at 37 °C, 5% CO_2), the infected wells were determined by hemagglutination [77]. The virus titer for all cases was calculated using the Reed-Muench method [78].

3.3. Analysis of Virus Degradation Using PCR Technique

Degradation of RNA molecules of influenza A/PR/8/34 (H1N1) virus was investigated using a PCR technique. Small pieces with an area of 4 cm^2 were cut from the prepared photoactive material and initial cotton fabric, used as a control, and placed in Petri dishes. A 150-µL aliquot of the culture medium containing virus was dropped on each piece, and Petri dishes with contaminated samples were covered with quartz glasses to prevent evaporation of liquid. One part of the dishes was irradiated using the UV–LED method mentioned above for 30, 60, 180, or 360 min to analyze the degradation of viral RNA using PCR. To analyze the effect of photoactive component on the degradation of virus, the second part of the dishes was stored simultaneously without irradiation. After time mentioned above, the samples were immersed into 2 mL of cold phosphate-buffered saline (PBS; Biolot) and vigorously shaken to rinse out the biological substances. The control point without irradiation (i.e., 0 min), when the samples were immersed in 2 mL of cold PBS immediately after dropping the culture medium containing virus on their surface, was performed to check the effect of adsorption of virus on the textile substrate. Then, 80-mL aliquots were sampled from all washouts, and an RNA extraction kit (Biolabmix, Novosibirsk, Russia) was used to isolate RNA molecules in test probes. The concentration of viral RNA in initial suspension and washouts from all the samples was analyzed by RT-qPCR method using "Seasonal Influenza Real-time RT-PCR Panel Primer and Probe Sets" (CDC, USA) in the reaction mix of HS-qPCR (2×) (Biolabmix). PCR tests were performed using a Light Cycler 96 (Roche Diagnostics, Rotkreuz, Switzerland). After completion of the reaction protocol, the threshold cycle value Cq was determined using Light Cycler 96 software (Roche Diagnostics, 1.1.0.1320 version) and used as a characteristic that correlates to concentration of RNA.

For statistical analysis at each irradiation time, at least three pieces of photoactive material and initial cotton fabric were tested independently to obtain an averaged Cq value. The total error was estimated as a standard deviation. A relative reduction in RNA concentration due to photocatalytic degradation was estimated using the $2^{-\Delta C_q'}$ method according to the published techniques [79,80].

4. Conclusions

The photoactive fabric is prepared via impregnation of cotton in isopropyl alcohol containing titanium isopropoxide as a binding agent and nanocrystalline TiO_2 as a photoactive component, followed by treatment of the material with water steam and drying at an increased temperature in air. The as-prepared cotton fabric exhibits strong absorption of UV light due to interband excitation of electrons in anatase TiO_2 nanocrystallites attached to cotton fibers and photocatalytic activity under corresponding radiation. Similar to the reference TiO_2 P25 photocatalyst, the photoactive fabric completely oxidizes acetone vapor under UV irradiation to CO_2 and water with a high rate, which indicates its high photocatalytic performance. In addition to low-molecular organic compounds, the prepared material is able to decompose the supramolecular structures and microorganisms. The

TCID$_{50}$ method confirms the inactivation of the influenza virus during the irradiation of the contaminated photoactive fabric with UV light of the A region. Virus adsorption and the rate of its inactivation increase as the concentration of protein in the virus suspension decreases due to lower competition between protein molecules and virus particles for adsorption sites on the surface of the photocatalyst. Long-term irradiation (3–6 h) results in the destruction of all virion structures to the point of RNA molecules, which are decomposed to fragments, with a number of nucleotides lower than 100 not to be detected using the PCR technique.

Supplementary Materials: The following are available online at https://www.mdpi.com/article/10.3390/catal12111298/s1, Figure S1: Adsorption kinetics of *E. coli* cells on the surface of cotton and photoactive fabrics; Figure S2: Dependence of virus titer on incubation time of contaminated cotton and photoactive fabrics without and with UV irradiation. Concentration of proteins in inoculum corresponds to 10 mg·mL^{-1}; Figure S3: Relative reduction in the concentration of virus RNA during the irradiation of photoactive and cotton-rich fabrics with blue light.

Author Contributions: D.S.: Methodology, Validation, Resources, Writing—original draft preparation, Writing—review and editing, Visualization; G.S.: Methodology, Validation, Resources, Writing—original draft preparation; M.S. (Mariia Sergeeva): Methodology, Investigation, Validation, Writing—original draft preparation; M.S. (Maria Solovyeva): Investigation, Writing—original draft preparation, Visualization; E.Z.: Investigation, Writing—original draft preparation; A.K.: Methodology, Resources; V.R.: Conceptualization, Resources; D.K.: Conceptualization, Supervision, Project administration, Funding acquisition. All authors have read and agreed to the published version of the manuscript.

Funding: The study was supported by the grant for the implementation of the strategic academic leadership program "Priority 2030" in Novosibirsk State University. The experiments on virus inactivation in Smorodintsev Research Institute of Influenza were supported by the Russian Foundation for Basic Research according to research project No. 18-29-17055.

Data Availability Statement: The data presented in this study are available on request from the corresponding author. The data are not publicly available due to privacy.

Acknowledgments: The experiments were performed using equipment of the Shared-Use Center "National Center for the Study of Catalysts" at the Boreskov Institute of Catalysis. The authors thank Maria Timofeeva from Smorodintsev Research Institute of Influenza for help in the experiments with influenza virus.

Conflicts of Interest: The authors declare no conflict of interest. The funders had no role in the design of the study; in the collection, analyses, or interpretation of data; in the writing of the manuscript; or in the decision to publish the results.

References

1. Ganesh, V.A.; Raut, H.K.; Nair, A.S.; Ramakrishna, S. A review on self-cleaning coatings. *J. Mater. Chem.* **2011**, *21*, 16304–16322. [CrossRef]
2. Sethi, S.K.; Manik, G. Recent Progress in Super Hydrophobic/Hydrophilic Self-Cleaning Surfaces for Various Industrial Applications: A Review. *Polym. Technol. Eng.* **2018**, *57*, 1932–1952. [CrossRef]
3. Wang, J.; Zhao, J.; Sun, L.; Wang, X. A review on the application of photocatalytic materials on textiles. *Text. Res. J.* **2014**, *85*, 1104–1118. [CrossRef]
4. Afzal, S.; Daoud, W.A.; Langford, S.J. Superhydrophobic and photocatalytic self-cleaning cotton. *J. Mater. Chem. A* **2014**, *2*, 18005–18011. [CrossRef]
5. Acayanka, E.; Tarkwa, J.-B.; Nchimi, K.N.; Voufouo, S.A.; Tiya-Djowe, A.; Kamgang, G.Y.; Laminsi, S. Grafting of N-doped titania nanoparticles synthesized by the plasma-assisted method on textile surface for sunlight photocatalytic self-cleaning applications. *Surfaces Interfaces* **2019**, *17*, 100361. [CrossRef]
6. Milošević, M.; Radoičić, M.; Šaponjić, Z.; Nunney, T.; Marković, D.; Nedeljković, J.; Radetić, M. In situ generation of Ag nanoparticles on polyester fabrics by photoreduction using TiO$_2$ nanoparticles. *J. Mater. Sci.* **2013**, *48*, 5447–5455. [CrossRef]
7. Nitayaphat, W.; Jirawongcharoen, P.; Trijaturon, T. Self-Cleaning Properties of Silk Fabrics Functionalized with TiO$_2$/SiO$_2$ Composites. *J. Nat. Fibers* **2017**, *15*, 262–272. [CrossRef]
8. Xing, H.; Cheng, J.; Tan, X.; Zhou, C.; Fang, L.; Lin, J. Ag nanoparticles-coated cotton fabric for durable antibacterial activity: Derived from phytic acid–Ag complex. *J. Text. Inst.* **2019**, *111*, 855–861. [CrossRef]

9. Xu, Q.; Ke, X.; Ge, N.; Shen, L.; Zhang, Y.; Fu, F.; Liu, X. Preparation of Copper Nanoparticles Coated Cotton Fabrics with Durable Antibacterial Properties. *Fibers Polym.* **2018**, *19*, 1004–1013. [CrossRef]

10. Molina, J. Graphene-based fabrics and their applications: A review. *RSC Adv.* **2016**, *6*, 68261–68291. [CrossRef]

11. Giachet, F.T.; Periolatto, M.; Ramirez, D.O.S.; Carletto, R.A.; Varesano, A.; Vineis, C.; Bongiovanni, R. Stability of ultraviolet-cured chitosan coating on cotton gauze for water filtration. *J. Ind. Text.* **2018**, *48*, 1384–1396. [CrossRef]

12. Gao, Y.; Cranston, R. Recent Advances in Antimicrobial Treatments of Textiles. *Text. Res. J.* **2008**, *78*, 60–72. [CrossRef]

13. Morais, D.S.; Guedes, R.M.; Lopes, M.A. Antimicrobial Approaches for Textiles: From Research to Market. *Materials* **2016**, *9*, 498. [CrossRef]

14. Grandcolas, M.; Sinault, L.; Mosset, F.; Louvet, A.; Keller, N.; Keller, V. Self-decontaminating layer-by-layer functionalized textiles based on WO3-modified titanate nanotubes. Application to the solar photocatalytic removal of chemical warfare agents. *Appl. Catal. A: Gen.* **2011**, *391*, 455–467. [CrossRef]

15. Yang, J.; Song, H.; Zhang, Y.; Zhu, X. Preparation of functionalization graphite carbonitride photocatalytic membrane and its application in degradation of organic pollutants. *Surfaces Interfaces* **2021**, *24*, 101092. [CrossRef]

16. Schneider, J.; Matsuoka, M.; Takeuchi, M.; Zhang, J.; Horiuchi, Y.; Anpo, M.; Bahnemann, D.W. Understanding TiO_2 Photocatalysis: Mechanisms and Materials. *Chem. Rev.* **2014**, *114*, 9919–9986. [CrossRef] [PubMed]

17. Soundarya, T.L.; Jayalakshmi, T.; Alsaiari, M.A.; Jalalah, M.; Abate, A.; Alharthi, F.A.; Ahmad, N.; Nagaraju, G. Ionic Liquid-Aided Synthesis of Anatase TiO_2 Nanoparticles: Photocatalytic Water Splitting and Electrochemical Applications. *Crystals* **2022**, *12*, 1133. [CrossRef]

18. Bakbolat, B.; Daulbayev, C.; Sultanov, F.; Beissenov, R.; Umirzakov, A.; Mereke, A.; Bekbaev, A.; Chuprakov, I. Recent Developments of TiO_2-Based Photocatalysis in the Hydrogen Evolution and Photodegradation: A Review. *Nanomaterials* **2020**, *10*, 1790. [CrossRef]

19. Som, I.; Roy, M. Recent development on titania-based nanomaterial for photocatalytic CO_2 reduction: A review. *J. Alloy. Compd.* **2022**, *918*. [CrossRef]

20. Al Jitan, S.; Palmisano, G.; Garlisi, C. Synthesis and Surface Modification of TiO_2-Based Photocatalysts for the Conversion of CO_2. *Catalysts* **2020**, *10*, 227. [CrossRef]

21. Zheng, H.; Zhang, S.; Liu, X.; O'Mullane, A.P. The application and improvement of TiO_2 (titanate) based nanomaterials for the photoelectrochemical conversion of CO_2 and N_2 into useful products. *Catal. Sci. Technol.* **2021**, *11*, 768–778. [CrossRef]

22. Yu, Z.; Liu, H.; Zhu, M.; Li, Y.; Li, W. Interfacial Charge Transport in 1D TiO_2 Based Photoelectrodes for Photoelectrochemical Water Splitting. *Small* **2019**, *17*, e1903378. [CrossRef] [PubMed]

23. Serga, V.; Burve, R.; Krumina, A.; Romanova, M.; Kotomin, E.; Popov, A. Extraction–Pyrolytic Method for TiO_2 Polymorphs Production. *Crystals* **2021**, *11*, 431. [CrossRef]

24. Mahy, J.; Lejeune, L.; Haynes, T.; Lambert, S.; Marcilli, R.; Fustin, C.-A.; Hermans, S. Eco-Friendly Colloidal Aqueous Sol-Gel Process for TiO_2 Synthesis: The Peptization Method to Obtain Crystalline and Photoactive Materials at Low Temperature. *Catalysts* **2021**, *11*, 768. [CrossRef]

25. Shayegan, Z.; Lee, C.-S.; Haghighat, F. TiO_2 photocatalyst for removal of volatile organic compounds in gas phase – A review. *Chem. Eng. J.* **2018**, *334*, 2408–2439. [CrossRef]

26. Barton, I.; Matejec, V.; Matousek, J. Photocatalytic activity of nanostructured TiO_2 coating on glass slides and optical fibers for methylene blue or methyl orange decomposition under different light excitation. *J. Photochem. Photobiol. A: Chem.* **2016**, *317*, 72–80. [CrossRef]

27. Selishchev, D.; Kolinko, P.; Kozlov, D. Adsorbent as an essential participant in photocatalytic processes of water and air purification: Computer simulation study. *Appl. Catal. A: Gen.* **2010**, *377*, 140–149. [CrossRef]

28. Ali, S.; Li, Z.; Chen, S.; Zada, A.; Khan, I.; Khan, I.; Ali, W.; Shaheen, S.; Qu, Y.; Jing, L. Synthesis of activated carbon-supported TiO_2-based nano-photocatalysts with well recycling for efficiently degrading high-concentration pollutants. *Catal. Today* **2019**, *335*, 557–564. [CrossRef]

29. Prorokova, N.P.; Kumeeva, T.Y.; Kuznetsov, O.Y. Antimicrobial Properties of Polyester Fabric Modified by Nanosized Titanium Dioxide. *Inorg. Mater. Appl. Res.* **2018**, *9*, 250–256. [CrossRef]

30. Pakdel, E.; Daoud, W.A.; Afrin, T.; Sun, L.; Wang, X. Self-cleaning wool: Effect of noble metals and silica on visible-light-induced functionalities of nano TiO_2 colloid. *J. Text. Inst.* **2015**, *106*, 1348–1361. [CrossRef]

31. Wang, P.; Dong, Y.; Li, B.; Li, Z.; Bian, L. A sustainable and cost effective surface functionalization of cotton fabric using TiO_2 hydrosol produced in a pilot scale: Condition optimization, sunlight-driven photocatalytic activity and practical applications. *Ind. Crop. Prod.* **2018**, *123*, 197–207. [CrossRef]

32. Selishchev, D.; Karaseva, I.; Uvaev, V.; Kozlov, D.; Parmon, V. Effect of preparation method of functionalized textile materials on their photocatalytic activity and stability under UV irradiation. *Chem. Eng. J.* **2013**, *224*, 114–120. [CrossRef]

33. Olak-Kucharczyk, M.; Szczepańska, G.; Kudzin, M.; Pisarek, M. The Photocatalytical Properties of RGO/TiO_2 Coated Fabrics. *Coatings* **2020**, *10*, 1041. [CrossRef]

34. Dong, Y.; Bai, Z.; Liu, R.; Zhu, T. Decomposition of indoor ammonia with TiO_2-loaded cotton woven fabrics prepared by different textile finishing methods. *Atmospheric Environ.* **2006**, *41*, 3182–3192. [CrossRef]

35. Wang, L.; Shen, Y.; Xu, L.; Cai, Z.; Zhang, H. Thermal crystallization of low-temperature prepared anatase nano-TiO_2 and multifunctional finishing of cotton fabrics. *J. Text. Inst.* **2015**, *107*, 651–662. [CrossRef]

36. Pakdel, E.; Daoud, W.A.; Sun, L.; Wang, X. Visible and UV functionality of TiO₂ ternary nanocomposites on cotton. *Appl. Surf. Sci.* **2014**, *321*, 447–456. [CrossRef]

37. Sobczyk-Guzenda, A.; Szymanowski, H.; Jakubowski, W.; Błasińska, A.; Kowalski, J.; Gazicki-Lipman, M. Morphology, photocleaning and water wetting properties of cotton fabrics, modified with titanium dioxide coatings synthesized with plasma enhanced chemical vapor deposition technique. *Surf. Coatings Technol.* **2013**, *217*, 51–57. [CrossRef]

38. Mihailović, D.; Saponjic, Z.; Radoicic, M.; Lazovic, S.; Baily, C.J.; Jovančić, P.; Nedeljkovic, J.; Radetić, M. Functionalization of cotton fabrics with corona/air RF plasma and colloidal TiO₂ nanoparticles. *Cellulose* **2011**, *18*, 811–825. [CrossRef]

39. Meilert, K.; Laub, D.; Kiwi, J. Photocatalytic self-cleaning of modified cotton textiles by TiO₂ clusters attached by chemical spacers. *J. Mol. Catal. A: Chem.* **2005**, *237*, 101–108. [CrossRef]

40. Foster, H.A.; Ditta, I.B.; Varghese, S.; Steele, A. Photocatalytic disinfection using titanium dioxide: Spectrum and mechanism of antimicrobial activity. *Appl. Microbiol. Biotechnol.* **2011**, *90*, 1847–1868. [CrossRef] [PubMed]

41. Rashid, M.M.; Simončič, B.; Tomšič, B. Recent advances in TiO₂-functionalized textile surfaces. *Surfaces Interfaces* **2020**, *22*, 100890. [CrossRef]

42. El-Ola, S.M.A.; Kotb, R.M.; Shaker, R.N. Photocatalytic finishing of silk and viscose fabrics. *J. Text. Inst.* **2020**, *112*, 820–827. [CrossRef]

43. Behzadnia, A.; Montazer, M.; Rad, M.M. Simultaneous sonosynthesis and sonofabrication of N-doped ZnO/TiO₂ core–shell nanocomposite on wool fabric: Introducing various properties specially nano photo bleaching. *Ultrason. Sonochemistry* **2015**, *27*, 10–21. [CrossRef]

44. Kangwansupamonkon, W.; Lauruengtana, V.; Surassmo, S.; Ruktanonchai, U. Antibacterial effect of apatite-coated titanium dioxide for textiles applications. *Nanomedicine: Nanotechnology, Biol. Med.* **2009**, *5*, 240–249. [CrossRef]

45. Rahal, R.; LE Bechec, M.; Guyoneaud, R.; Pigot, T.; Paolacci, H.; Lacombe, S. Bactericidal activity under UV and visible light of cotton fabrics coated with anthraquinone-sensitized TiO₂. *Catal. Today* **2013**, *209*, 134–139. [CrossRef]

46. Zahid, M.; Papadopoulou, E.L.; Suarato, G.; Binas, V.D.; Kiriakidis, G.; Gounaki, I.; Moira, O.; Venieri, D.; Bayer, I.S.; Athanassiou, A. Fabrication of Visible Light-Induced Antibacterial and Self-Cleaning Cotton Fabrics Using Manganese Doped TiO₂ Nanoparticles. *ACS Appl Bio Mater* **2018**, *1*, 1154–1164. [CrossRef] [PubMed]

47. Ganguly, P.; Byrne, C.; Breen, A.; Pillai, S.C. Antimicrobial activity of photocatalysts: Fundamentals, mechanisms, kinetics and recent advances. *Appl. Catal. B: Environ.* **2018**, *225*, 51–75. [CrossRef]

48. Kowalczyk, D.; Brzeziński, S.; Kaminska, I. Multifunctional nanocoating finishing of polyester/cotton woven fabric by the sol-gel method. *Text. Res. J.* **2017**, *88*, 946–956. [CrossRef]

49. Behzadnia, A.; Montazer, M.; Rashidi, A.; Rad, M.M. Rapid Sonosynthesis of N-Doped Nano TiO₂ on Wool Fabric at Low Temperature: Introducing Self-cleaning, Hydrophilicity, Antibacterial/Antifungal Properties with low Alkali Solubility, Yellowness and Cytotoxicity. *Photochem. Photobiol.* **2014**, *90*, 1224–1233. [CrossRef]

50. Mazurkova, N.A.; Spitsyna, Y.E.; Shikina, N.V.; Ismagilov, Z.R.; Zagrebel'Nyi, S.N.; Ryabchikova, E.I. Interaction of titanium dioxide nanoparticles with influenza virus. *Nanotechnologies Russ.* **2010**, *5*, 417–420. [CrossRef]

51. Cui, H.; Jiang, J.; Gu, W.; Sun, C.; Wu, D.; Yang, T.; Yang, G. Photocatalytic Inactivation Efficiency of Anatase Nano-TiO₂ Sol on the H₉N₂ Avian Influenza Virus. *Photochem. Photobiol.* **2010**, *86*, 1135–1139. [CrossRef] [PubMed]

52. Kozlova, E.A.; Safatov, A.S.; Kiselev, S.A.; Marchenko, V.Y.; Sergeev, A.A.; Skarnovich, M.O.; Emelyanova, E.K.; Smetannikova, M.A.; Buryak, G.A.; Vorontsov, A.V. Inactivation and Mineralization of Aerosol Deposited Model Pathogenic Microorganisms over TiO₂ and Pt/TiO₂. *Environ. Sci. Technol.* **2010**, *44*, 5121–5126. [CrossRef]

53. Monmaturapoj, N.; Sri-On, A.; Klinsukhon, W.; Boonnak, K.; Prahsarn, C. Antiviral activity of multifunctional composite based on TiO₂-modified hydroxyapatite. *Mater. Sci. Eng. C* **2018**, *92*, 96–102. [CrossRef] [PubMed]

54. Manivannan, R.; Park, S.H.; Ryu, J.; Park, J.-Y.; Shin, H.-J.; Son, Y.-A. Ultrasonic assisted surface modified cellulose: Photocatalytic effect for the disinfection of microbes using porphyrin dyes. *Dye. Pigment.* **2022**, *204*. [CrossRef]

55. Kim, M.G.; Kang, J.M.; Lee, J.E.; Kim, K.S.; Kim, K.H.; Cho, M.; Lee, S.G. Effects of Calcination Temperature on the Phase Composition, Photocatalytic Degradation, and Virucidal Activities of TiO₂ Nanoparticles. *ACS Omega* **2021**, *6*, 10668–10678. [CrossRef] [PubMed]

56. Nakano, R.; Ishiguro, H.; Yao, Y.; Kajioka, J.; Fujishima, A.; Sunada, K.; Minoshima, M.; Hashimoto, K.; Kubota, Y. Photocatalytic inactivation of influenza virus by titanium dioxide thin film. *Photochem. Photobiol. Sci.* **2012**, *11*, 1293–1298. [CrossRef] [PubMed]

57. Han, R.; Coey, J.D.; O'Rourke, C.; Bamford, C.G.; Mills, A. Flexible, disposable photocatalytic plastic films for the destruction of viruses. *J. Photochem. Photobiol. B: Biol.* **2022**, *235*, 112551. [CrossRef]

58. Nakano, R.; Hara, M.; Ishiguro, H.; Yao, Y.; Ochiai, T.; Nakata, K.; Murakami, T.; Kajioka, J.; Sunada, K.; Hashimoto, K.; et al. Broad Spectrum Microbicidal Activity of Photocatalysis by TiO₂. *Catalysts* **2013**, *3*, 310–323. [CrossRef]

59. Choi, S.-Y.; Cho, B. Extermination of influenza virus H1N1 by a new visible-light-induced photocatalyst under fluorescent light. *Virus Res.* **2018**, *248*, 71–73. [CrossRef] [PubMed]

60. Hajkova, P.; Spatenka, P.; Horsky, J.; Horska, I.; Kolouch, A. Photocatalytic Effect of TiO₂ Films on Viruses and Bacteria. *Plasma Process. Polym.* **2007**, *4*, S397–S401. [CrossRef]

61. Lee, J.E.; Ko, G. Norovirus and MS2 inactivation kinetics of UV-A and UV-B with and without TiO₂. *Water Res.* **2013**, *47*, 5607–5613. [CrossRef]

62. Markowska-Szczupak, A.; Ulfig, K.; Morawski, A. The application of titanium dioxide for deactivation of bioparticulates: An overview. *Catal. Today* **2011**, *169*, 249–257. [CrossRef]

63. Jafry, H.R.; Liga, M.V.; Li, Q.; Barron, A.R. Simple Route to Enhanced Photocatalytic Activity of P25 Titanium Dioxide Nanoparticles by Silica Addition. *Environ. Sci. Technol.* **2010**, *45*, 1563–1568. [CrossRef] [PubMed]

64. Ishiguro, H.; Nakano, R.; Yao, Y.; Kajioka, J.; Fujishima, A.; Sunada, K.; Minoshima, M.; Hashimoto, K.; Kubota, Y. Photocatalytic inactivation of bacteriophages by TiO2-coated glass plates under low-intensity, long-wavelength UV irradiation. *Photochem. Photobiol. Sci.* **2011**, *10*, 1825–1829. [CrossRef] [PubMed]

65. Yamaguchi, Y.; Shimodo, T.; Usuki, S.; Torigoe, K.; Terashima, C.; Katsumata, K.-I.; Ikekita, M.; Fujishima, A.; Sakai, H.; Nakata, K. Different hollow and spherical TiO_2 morphologies have distinct activities for the photocatalytic inactivation of chemical and biological agents. *Photochem. Photobiol. Sci.* **2016**, *15*, 988–994. [CrossRef] [PubMed]

66. Zheng, X.; Shen, Z.-P.; Cheng, C.; Shi, L.; Cheng, R.; Yuan, D.-H. Photocatalytic disinfection performance in virus and virus/bacteria system by $Cu-TiO_2$ nanofibers under visible light. *Environ. Pollut.* **2018**, *237*, 452–459. [CrossRef] [PubMed]

67. Mostafa, A.; Abdelwhab, E.M.; Mettenleiter, T.C.; Pleschka, S. Zoonotic Potential of Influenza A Viruses: A Comprehensive Overview. *Viruses* **2018**, *10*, 497. [CrossRef]

68. French, A.D. Idealized powder diffraction patterns for cellulose polymorphs. *Cellulose* **2013**, *21*, 885–896. [CrossRef]

69. Wu, D.; Long, M. Low-temperature synthesis of $N-TiO_2$ sol and characterization of $N-TiO_2$ coating on cotton fabrics. *Surf. Coatings Technol.* **2012**, *206*, 3196–3200. [CrossRef]

70. Sobczyk-Guzenda, A.; Owczarek, S.; Szymanowski, H.; Gazicki-Lipman, M. Amorphous and crystalline TiO_2 coatings synthesized with the RF PECVD technique from metalorganic precursor. *Vacuum* **2015**, *117*, 104–111. [CrossRef]

71. Selishchev, D.; Kolobov, N.; Pershin, A.; Kozlov, D. TiO_2 mediated photocatalytic oxidation of volatile organic compounds: Formation of CO as a harmful by-product. *Appl. Catal. B: Environ.* **2017**, *200*, 503–513. [CrossRef]

72. Bono, N.; Ponti, F.; Punta, C.; Candiani, G. Effect of UV Irradiation and TiO_2-Photocatalysis on Airborne Bacteria and Viruses: An Overview. *Materials* **2021**, *14*, 1075. [CrossRef]

73. Matsuura, R.; Lo, C.-W.; Wada, S.; Somei, J.; Ochiai, H.; Murakami, T.; Saito, N.; Ogawa, T.; Shinjo, A.; Benno, Y.; et al. SARS-CoV-2 Disinfection of Air and Surface Contamination by TiO_2 Photocatalyst-Mediated Damage to Viral Morphology, RNA, and Protein. *Viruses* **2021**, *13*, 942. [CrossRef] [PubMed]

74. Kovalevskiy, N.; Selishchev, D.; Svintsitskiy, D.; Selishcheva, S.; Berezin, A.; Kozlov, D. Synergistic effect of polychromatic radiation on visible light activity of N-doped TiO_2 photocatalyst. *Catal. Commun.* **2020**, *134*. [CrossRef]

75. Solovyeva, M.; Selishchev, D.; Cherepanova, S.; Stepanov, G.; Zhuravlev, E.; Richter, V.; Kozlov, D. Self-cleaning photoactive cotton fabric modified with nanocrystalline TiO_2 for efficient degradation of volatile organic compounds and DNA contaminants. *Chem. Eng. J.* **2020**, *388*, 124167. [CrossRef]

76. Kovalevskiy, N.; Selishcheva, S.; Solovyeva, M.; Selishchev, D. In situ IR spectroscopy data and effect of the operational parameters on the photocatalytic activity of N-doped TiO_2. *Data Brief* **2019**, *24*, 103917. [CrossRef] [PubMed]

77. Hirst, G.K. The quantitative determination of influenza virus and antibodies by means of red cell agglutination. *J. Exp. Med.* **1942**, *75*, 49–64. [CrossRef] [PubMed]

78. Reed, L.J.; Muench, H. A simple method of estimating fifty per cent endpoints. *Am. J. Epidemiol.* **1938**, *27*, 493–497. [CrossRef]

79. Livak, K.J.; Schmittgen, T.D. Analysis of relative gene expression data using real-time quantitative PCR and the $2^{-\Delta\Delta CT}$ Method. *Methods* **2001**, *25*, 402–408. [CrossRef] [PubMed]

80. Dorak, M.T. *Real-Time PCR*; Taylor & Francis Group: Abingdon, UK, 2006.